atmosphere

MDPI

Article

Spatiotemporal Exposure Assessment of $PM_{2.5}$ Concentration Using a Sensor-Based Air Monitoring System

Jihun Shin, Jaemin Woo, Youngtae Choe, Gihong Min, Dongjun Kim, Daehwan Kim, Sanghoon Lee and Wonho Yang *

Department of Health & Safety, Daegu Catholic University, Gyeongsan 38430, Republic of Korea; shinjs1130@naver.com (J.S.); toddlf3dnjf@naver.com (J.W.); kickilbo@naver.com (Y.C.); alsrlghd000@naver.com (G.M.); rlaehdwns3739@naver.com (D.K.); eorkfdl99@naver.com (D.K.); sanghoon8474@daum.net (S.L.)

* Correspondence: whyang@cu.ac.kr

Abstract: Sensor-based air monitoring instruments (SAMIs) can provide high-resolution air quality data by offering a detailed mapping of areas that air quality monitoring stations (AQMSs) cannot reach. This enhances the precision of estimating $PM_{2.5}$ concentration levels for areas that have not been directly measured, thereby enabling an accurate assessment of exposure. The study period was from 30 September to 2 October 2019 in the Guro-gu district, Seoul, Republic of Korea. Four models were applied to assess the suitability of the SAMIs and visualize the temporal and spatial distribution of $PM_{2.5}$. Assuming that the $PM_{2.5}$ concentrations measured at a SAMI located in the center of the Guro-gu district represent the true values, the $PM_{2.5}$ concentrations estimated using QGIS spatial interpolation techniques were compared. The SAMIs were used at seven points (S_1–S_7) according to the distance. Models 3 and 4 accurately estimated the unmeasured points with higher coefficients of determination (R^2) than the other models. As the distance from the AQMS increased from S_1 to S_7, the R^2 between the observed and estimated values decreased from 0.89 to 0.29, respectively. The auxiliary installation of SAMIs could resolve regional concentration imbalances, allowing for the accurate estimation of pollutant concentrations and improved risk assessment for the population.

Keywords: $PM_{2.5}$; sensor-based instruments; interpolation; spatiotemporal resolution; population exposure

Citation: Shin, J.; Woo, J.; Choe, Y.; Min, G.; Kim, D.; Kim, D.; Lee, S.; Yang, W. Spatiotemporal Exposure Assessment of $PM_{2.5}$ Concentration Using a Sensor-Based Air Monitoring System. *Atmosphere* **2024**, *15*, 664. https://doi.org/10.3390/atmos15060664

Academic Editors: Christos Argyropoulos, Zoi Dorothea Pana and Changqing Lin

Received: 25 April 2024
Revised: 26 May 2024
Accepted: 29 May 2024
Published: 31 May 2024

1. Introduction

Air pollution can have significant adverse effects on human health. The World Health Organization (WHO) has reported that nine out of 10 people worldwide breathe air containing high levels of pollutants, and approximately 7 million people die prematurely every year due to air pollution [1]. Among these, fine particulate matter ($PM_{2.5}$) is the main risk factor [2]. The International Agency for Research on Cancer has designated $PM_{2.5}$ as a Group 1 human carcinogen, which can cause cancer [3]. $PM_{2.5}$ adversely affects health, causing respiratory diseases, such as asthma and chronic obstructive pulmonary disease, cardiovascular diseases, skin diseases, and allergies [4]. Therefore, it is important to recognize the adverse effects of atmospheric $PM_{2.5}$ and develop strategies to manage exposure in the general population.

The Korean Ministry of Environment has operated an air quality monitoring station (AQMS) throughout the country since 1995 to determine whether national air pollution and air quality standards have been met. In addition, Air Korea (www.airkorea.or.kr (accessed on 1 April 2024)) provides exposure information to air pollutants by providing real-time air quality information measured by the AQMS to the public in the form of the air quality index through the Internet and smartphones. In previous epidemiological and risk assessment studies, the $PM_{2.5}$ concentration produced by AQMSs was used to compare mortality or human effects in the area or analyze correlations between population and prevalence of

asthma, cardiovascular disease, and other diseases [5–7]. These monitoring stations may provide accurate and reliable data on air quality in a specific area [8]. However, the AQMSs cannot accurately assess personal or population exposure owing to spatial constraints, resulting in lower accuracy for air pollutants far from the monitoring station. Therefore, even though AQMS provides accurate data, it cannot explain important local variations crucial for public health protection in detail [9,10]. In addition, there is a limitation to increasing the spatial density owing to the high cost of additional installations.

Currently, the trend to increase air quality data collection using a variety of methodologies other than AQMS has been growing globally. Sensor platforms for monitoring a variety of air pollutants are accessible, and new devices in this field are constantly being released [11]. In recent years, many studies using sensor-based air monitoring instruments (SAMIs) have been conducted to address the spatial limitations of existing AQMSs [12–14]. SAMIs can provide high-resolution air quality data by providing a more detailed mapping of areas that AQMSs cannot reach [15].

Owing to the nature of air pollutants, it is important to increase their spatiotemporal resolution because the influence of pollutants varies from region to region, and their distribution might not be uniform. This improvement in spatiotemporal resolution can increase the accuracy of concentration estimations for unmeasured points in modeling methods, such as Geographic Information Systems (GIS).

The objectives of this study were to enhance spatiotemporal resolution by complementing the spatial constraints of AQMSs through the auxiliary installation of SAMIs and to utilize this setup to improve the accuracy of $PM_{2.5}$ concentration estimation for unmeasured points. This enhances the precision of estimating $PM_{2.5}$ concentration levels for areas that have not been directly measured, thus enabling accurate assessments of exposure. This manuscript was organized to estimate the spatiotemporal concentrations using SAMIs and QGIS and to provide an optimal installation distance through a comparison of applied models.

2. Materials and Methods

2.1. Target Area and Locations of SAMIs and AQMSs

The study area was the Guro-gu district, Seoul, Republic of Korea (Figure 1). It had a population of 444,146 in January 2020, accounting for 4.2% of the population of Seoul, with an area of 20.12 km^2. Four models were applied using AQMSs and SAMIs for the temporal and spatial visualization of $PM_{2.5}$, respectively. Model 1 consisted of only an AQMS at a single point, and Model 2 was configured by installing an AQMS in nearby areas to Model 1. Model 3 used data from only SAMIs, and Model 4 was combined with all other models. The first model (Model 1) consisted of one AQMS, and the second model (Model 2) consisted of nearby air quality monitoring stations (NAQMSs), with a combination of one AQMS and 11 suburban AQMSs. The third model (Model 3) consisted of 22 SAMI locations, and near a sensor-based air monitoring instrument consisting of 34 locations combining NAQMS and SAMI was the fourth model (Model 4) (Figure 2). All the measurement station locations were collected by converting the addresses into latitude and longitude coordinates.

Figure 1. Location of the study area.

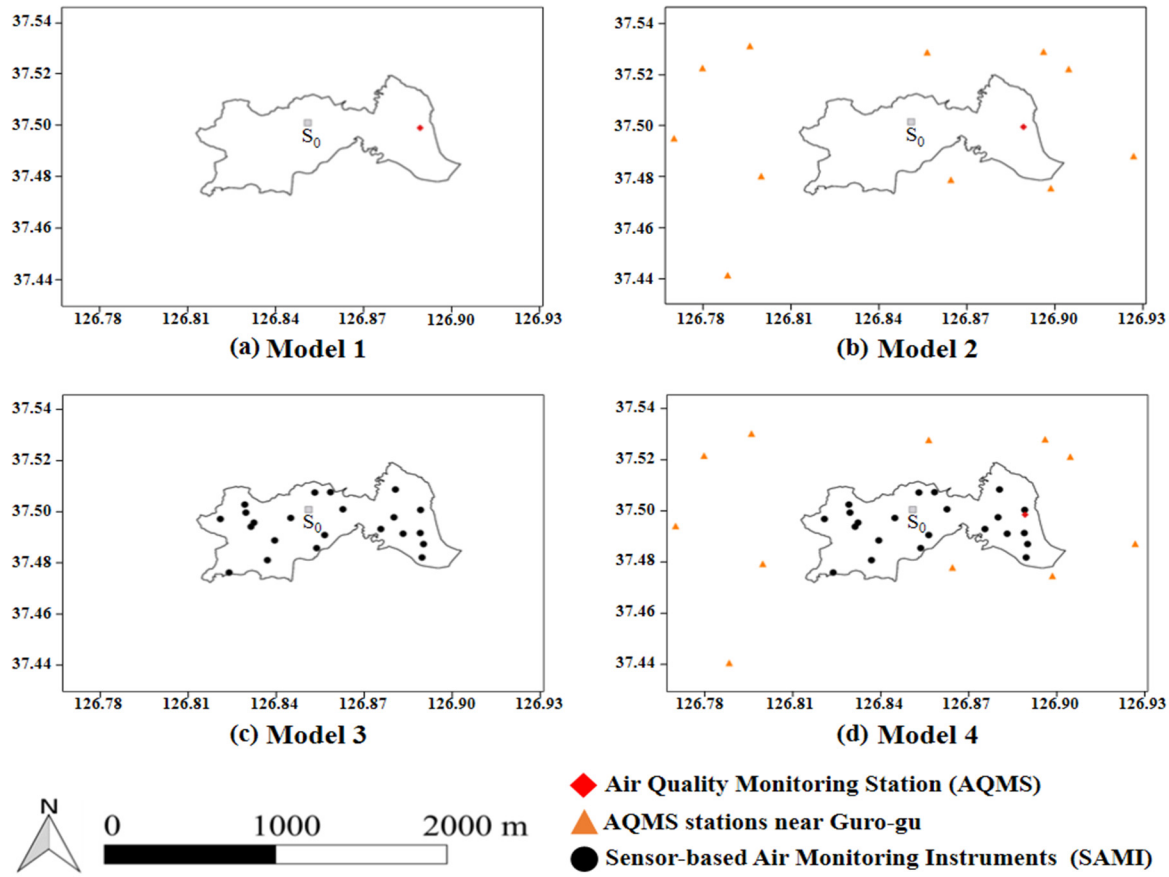

Figure 2. Measurement points of AQMSs and SAMIs according to the four kinds of models.

2.2. $PM_{2.5}$ Concentration Measurement

Outdoor $PM_{2.5}$ concentrations, measured at one AQMS in the Guro district and 11 nearby AQMSs, were collected from the data provided by Air Korea (www.airkorea.or.kr (accessed on 30 September 2019)) of the Ministry of Environment, as shown in Figure 2. The $PM_{2.5}$ concentrations measured by the SAMIs were collected every minute and transmitted to the Government Cloud (G-Cloud), which is a cloud computing service developed for the Korean government's public institution and launched in 2012 [16]. The collection period for all data was real-time concentration.

The collection period of all data was a real-time concentration in 1 h units from 30 September to 2 October 2019. The principle of $PM_{2.5}$ concentration measurement by SAMI was the light scattering spectrometer, and the specification was a sensor model of SD-16C (Dust Mon, Sentry Co., Ltd., Seoul, Republic of Korea), a flow rate of 0.5 L/min, and a resolution of 0.1 $\mu g/m^3$. The comprehensive specifications of the SAMI are shown in Figure 3.

This instrument in SAMIs was designed to maintain a temperature of 20 °C and a relative humidity of less than 70% with a pretreatment control device and an integrated system because of measurement errors that may occur due to various environmental factors, as shown in Figure 3. In our previous study, it was found that for the accuracy of the $PM_{2.5}$ concentration, the coefficient of determination (R^2) was 0.96, obtained through a co-location test comparing the values monitored by installing a sensor-based measuring instrument in the same location as the air pollution monitoring station [17]. Therefore, among the SAMIs installed in Guro-gu, we considered S_0, located at the central point, to be equivalent to the AQMS, as shown in Figure 2. Compared with AQMSs, SAMIs provided slightly lower observed values, and the data were applied without applying a separate correction factor. For all $PM_{2.5}$ concentration data, outliers were removed using the interquartile range to increase the reliability of the values [18].

$PM_{2.5}$ sensor model	SD-16C (Republic of Korea)
Measuring principle	Light scattering spectrometer
Measuring range	PM: 0 ~ 1000 mg/m^3
	Temperature: −40 ~ 80°C
	Humidity: 0 ~ 100% RH
Pump method	Diaphragm pump
Particle size range	0.3 ~ 25 μm
Reproducibility	±5%
Flow rate	0.5 L/min
Resolution	0.1 μg/m^3
Coefficient of determination with AQMS	R^2 = 0.96

Figure 3. Specification of the SAMI (sensor-based air monitoring instrument) used in this study.

2.3. Spatial Interpolation

An interpolation methodology using GIS was used to estimate the $PM_{2.5}$ concentration at unmeasured points. GIS provides information, such as maps, pictures, and diagrams, through the location data of objects with geographical locations and attribute data, which include information on the characteristics of those locations. For spatial modeling, the outdoor daily average $PM_{2.5}$ concentration was calculated and used as attribute data, and the satellite coordinate system (WGS-84) of the location where the SAMI was installed in each region was used as the location data. Three spatial interpolation techniques were used: Inverse Distance Weighted (IDW), Ordinary Kriging (OK), and Universal Kriging (UK). The IDW technique was interpolated and visualized using the open-source program QGIS (version 3.22), and the kriging was interpolated for 1 h using the open-source program SAGA GIS (version 7.8.2) and visualized using QGIS.

2.4. Model Evaluation via Spatial Analysis

One station (S_0) was selected from among the measurement stations located at the center of the Guro-gu district, as shown in Figure 2. Based on the AQMS points located in the Guro-gu district, seven stations (S_1–S_7) were selected based on the distance to the SAMI. The distance from station 1 to station 7 ranges from 1.4 km to 6.3 km, as shown in Figure 4. Verification was compared to the estimated value of S_0 using the four models mentioned above. Three statistical analyses were performed to confirm the accuracy: coefficient of determination (R^2), root mean squared error (RMSE), and mean absolute error (MAE).

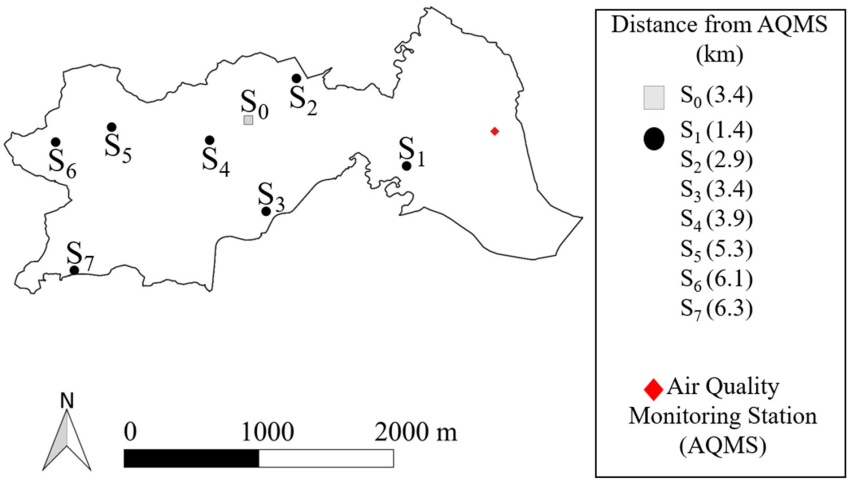

Figure 4. Selection of SAMI (S_1–S_7) to evaluate $PM_{2.5}$ concentration estimation accuracy according to the distance from AQMS.

3. Results

3.1. $PM_{2.5}$ Concentrations According to the Models

The distribution of $PM_{2.5}$ concentrations, measured according to each model, is shown in Figure 5. As a result of analyzing the concentration of $PM_{2.5}$ observed on 30 September, Model 1 showed the lowest value among the four models at 29.6 ± 10.9 μg/m^3. Average $PM_{2.5}$ concentrations in Models 3, 4, and 2 were 62.6 ± 33.6 μg/m^3, 55.3 ± 27.7 μg/m^3, and 48.9 ± 19.1 μg/m^3, respectively. The maximum value was 50.0 μg/m^3 in Model 1 and 152.0 μg/m^3 in Model 3, indicating a difference of approximately 100 μg/m^3. On 1 October, Model 1 showed the lowest value at 22.8 ± 8.3 μg/m^3, while Model 2 showed the highest value at 42.7 ± 22.0 μg/m^3. The median value was approximately 3–7 μg/m^3 lower than the average value. The maximum value observed in Models 2 and 4, which combined nearby measuring stations, was 122.0 μg/m^3. The concentration on 2 October was half the average concentration of that on the previous two days, and Model 1 had the lowest reading at 9.8 ± 8.2 μg/m^3. The other models exhibited values close to 19.0 μg/m^3.

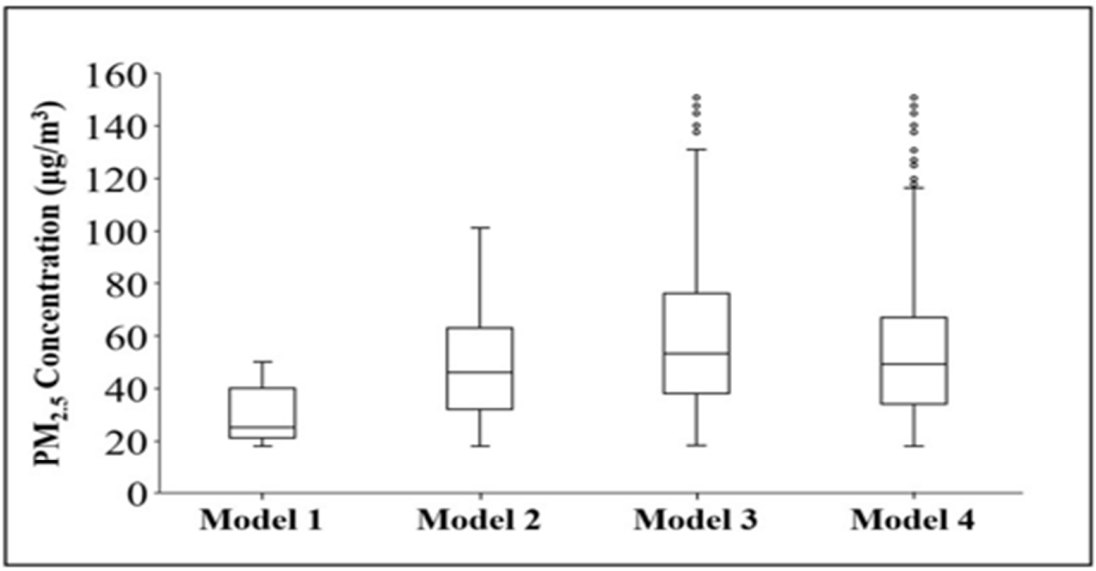

(a) September 30th

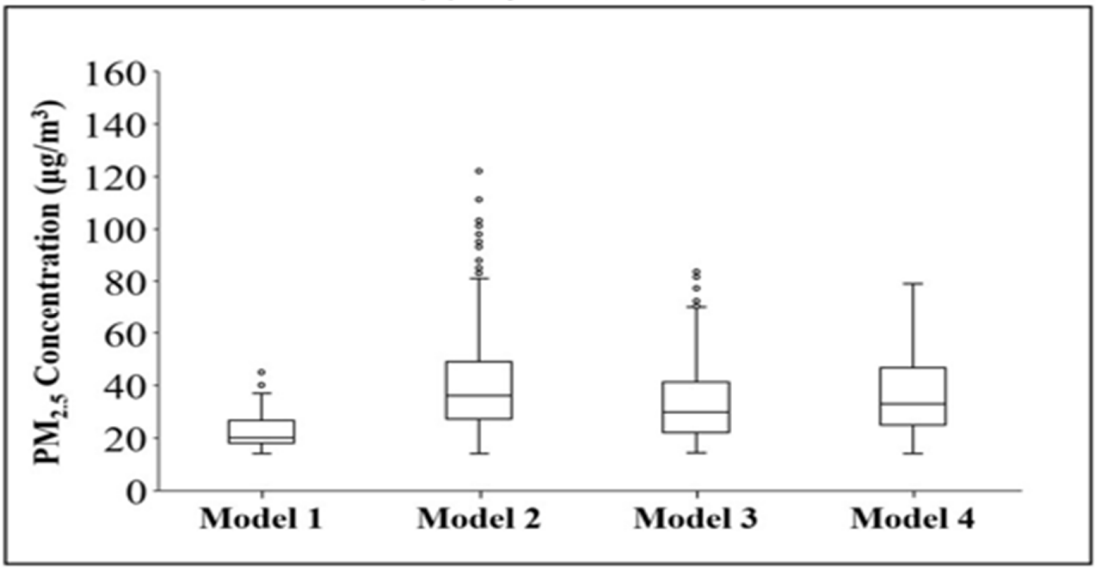

(b) October 1st

Figure 5. *Cont.*

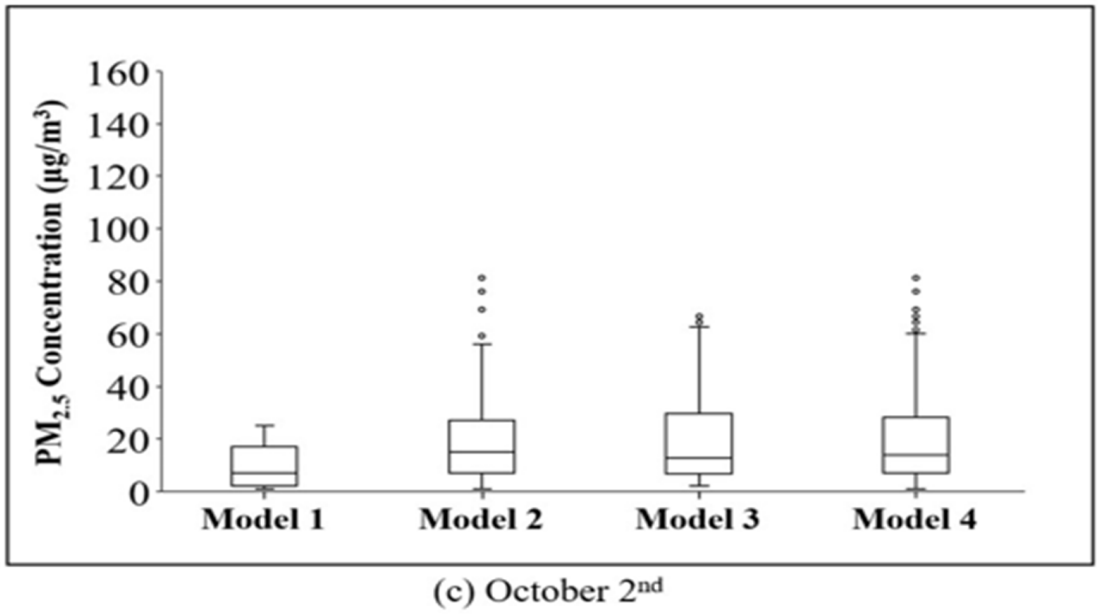

Figure 5. Distribution of $PM_{2.5}$ concentrations according to each model.

3.2. Verification between Estimation and Observation

The accuracy of each model was evaluated via statistical verification by comparing the measured values obtained from the central monitoring station in the Guro district (S_0) with the values estimated via interpolation in each model. The interpolation results for each estimation method at 13:00 on 30 September are shown in Figure 6. Model 1 was interpolated at a single point, resulting in R^2, RMSE, and MAE values of 0.66, 45.0 μg/m^3, and 34.0 μg/m^3, respectively. These values remained consistent across all the interpolation methods. The R^2 increased or remained similar as the number of measurement points increased using the IDW technique, whereas the RMSE and MAE decreased, indicating an improvement in the accuracy of the model. Similar to the IDW technique, the accuracy of the model improved as the number of measurement points increased, even when the OK technique was used for statistical validation. The R^2 of Model 3 was 0.95, which was similar to that of Model 4, which included the monitoring stations in the vicinity. Model 3 was the most accurate in predicting S_0, with an RMSE of 13.6 μg/m^3 and an MAE of 8.9 μg/m^3. The UK technique showed that the R^2 values for Model 1 and Model 2, considering AQMSs, were 0.66 and 0.63, respectively. The corresponding RMSE values were 45.0 and 34.9. Models 3 and 4, considering the SAMIs, had the same results as OK, as shown in Table 1.

Table 1. Comparison of statistical verification (R^2, RMSE, and MAE) for each interpolation technique for S_0.

Interpolation	Validation	Model			
		Model 1 (*n* = 48)	**Model 2 (*n* = 49)**	**Model 3 (*n* = 49)**	**Model 4 (*n* = 49)**
Inverse Distance Weighted (IDW)	R^2 *	0.66	0.63	0.94	0.93
	RMSE **	45.0	35.5	17.2	19.0
	MAE ***	34.0	22.6	11.5	12.7
Ordinary Kriging (OK)	R^2	0.66	0.66	0.95	0.95
	RMSE	45.0	34.6	13.6	13.9
	MAE	34.0	22.1	8.9	9.1
Universal Kriging (UK)	R^2	0.66	0.63	0.95	0.95
	RMSE	45.0	34.9	13.6	13.9
	MAE	34.0	22.3	8.9	9.1

* Coefficient of determination; ** Root mean square error; *** Mean absolute error.

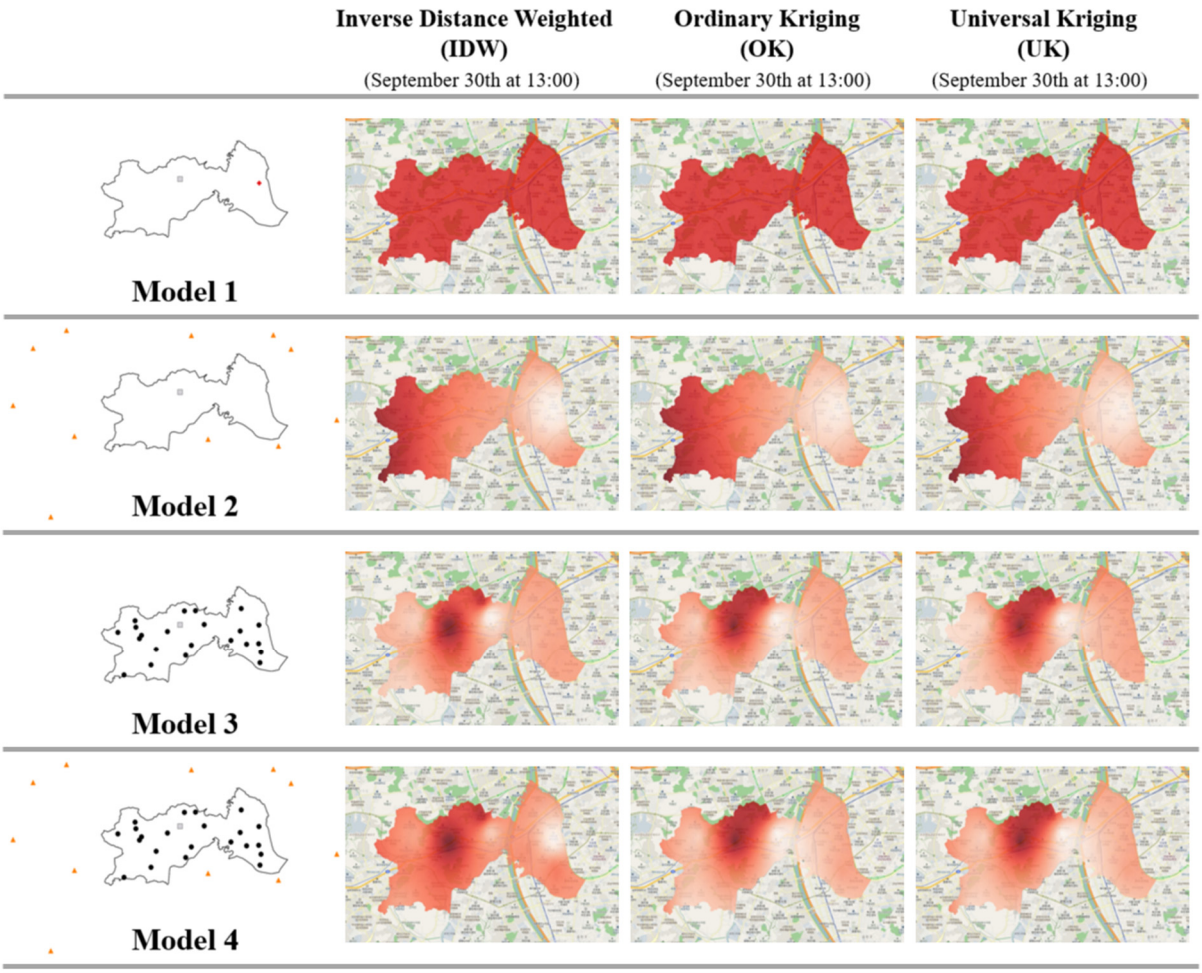

Figure 6. Visualization of $PM_{2.5}$ concentration estimated according to the four kinds of models.

3.3. Comparison by SAMIs According to Distance from the AQMSs

The correlations between SAMIs (S_1–S_7) according to the distance from the AQMSs in the Guro-gu district through each spatial interpolation technique were compared using OK (Figure 7). S_1 and S_2 present the scatter plot of R^2 derived using the IDW and UK method, respectively.

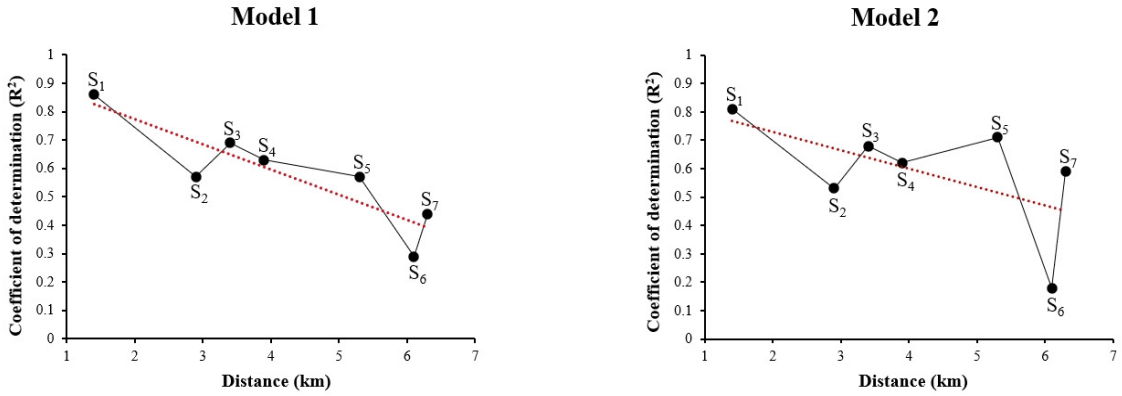

Figure 7. *Cont.*

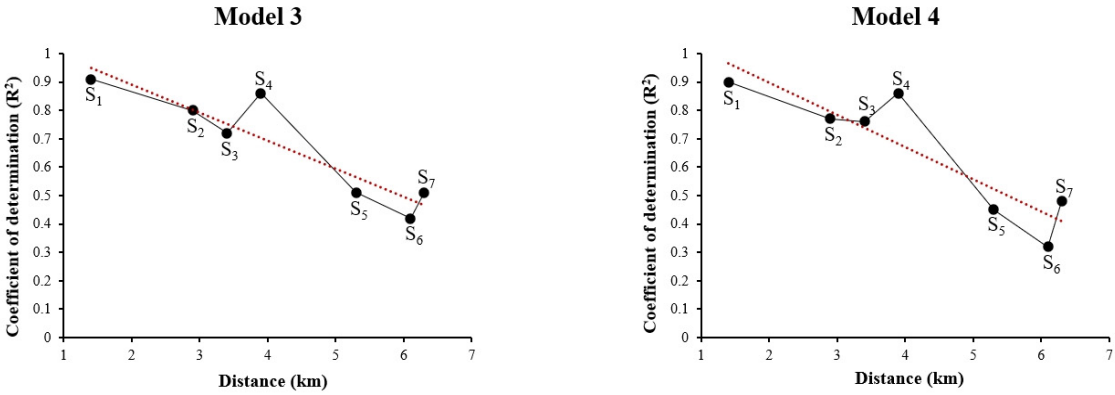

Figure 7. Scatter plot of the coefficient of determination derived using the Ordinary Kriging (OK) method for S_1–S_7 according to distance from the AQMS.

Among the AQMSs and SAMIs, the R^2 of the monitoring station (S_1) located at 1.4 km was the highest at 0.81–0.91, and Model 3 showed the highest R^2 at 0.91. Monitoring stations (S_2–S_4) within a 2 km radius in Model 3, which includes a SAMI with a relatively large number of monitoring stations, recorded relatively high R^2 values of 0.80, 0.72, and 0.86. Although there was a difference in the R^2 values according to the classification of the monitoring station, the trend of the graph decreased in all four models as the distance from the AQMSs increased.

4. Discussion

This study was conducted to confirm whether the auxiliary installation of a SAMI overcomes the limitations of the existing AQMSs and improves the accuracy of calculating local residents' exposure to $PM_{2.5}$. After classifying the four models using AQMSs and SAMIs, the $PM_{2.5}$ concentrations measured were collected at the measurement stations of each model. Spatial interpolation techniques, such as IDW and kriging, were performed through the QGIS program to visualize the $PM_{2.5}$ concentration using the collected $PM_{2.5}$ concentration, and the concentration for unmeasured points was estimated. The estimated values obtained through interpolation were statistically verified by the comparison with the observed values measured using SAMIs (S_0).

The AQMS is limited in its ability to measure air quality beyond a certain distance, which can reduce the accuracy of exposure assessments. In addition, owing to cost constraints, the spatial resolution cannot be increased. Therefore, installing a SAMI as an auxiliary installation could overcome spatial limitations at a relatively low cost and address the limitations of an AQMS by collecting more data on $PM_{2.5}$ concentrations. In this study, cross validation was performed for each interpolation technique to compare and evaluate the accuracy of the models.

In previous epidemiological studies, $PM_{2.5}$ concentrations measured at the AQMSs were estimated through spatial interpolation using GIS and subsequently utilized for exposure assessment [19]. Spatial interpolation is a technique that estimates the values of unobserved points using the values of observed points. It can be used to predict the concentration of air pollutants in a range that cannot be measured using an AQMS [20]. The accuracy of this process depends on the precision, quantity, and distribution of known points [21]. In a study conducted in Delhi, India, pollutants generated from vehicles were visualized using the kriging technique in GIS. Subsequently, respiratory and cardiovascular deaths were estimated based on exposure to air pollutants [22]. Spatial interpolation was used to evaluate the efficacy of monitoring sites located in Seoul, Republic of Korea, and to validate the accuracy of atmospheric $PM_{2.5}$ concentration measurements. These results indicate that additional monitoring stations are required for high-resolution monitoring [23]. In a study utilizing wind-field data, the spatial interpolation results were significantly enhanced compared with conventional methods, demonstrating the effectiveness of

incorporating meteorological factors into $PM_{2.5}$ concentration estimations [24]. Similarly, research on regional $PM_{2.5}$ concentration estimation found that using optimized spatial models with radial basis function interpolation greatly improved prediction accuracy [25]. These findings suggest the potential for advancing interpolation techniques through various innovative approaches.

Similar to previous studies, this study also demonstrates the potential of overcoming the limitations of the measurement imbalance between AQMS regions by predicting the concentration in unmeasured regions through spatial interpolation. The auxiliary installation of SAMIs has the potential to improve the accuracy of forecasting ambient $PM_{2.5}$ levels and reduce costs by overcoming the limitations of the AQMSs. Several studies have conducted comparative evaluations to assess the accuracy of both the AQMSs and SAMIs [26].

In a previous study conducted in December 2018 to ensure the accuracy of SAMI, we conducted a co-location test with AQMS at the site S_0 over approximately 334 h across 15 days, resulting in a correlation coefficient (R^2) of 0.96 [17]. Although the SAMIs were only placed outdoors at public buildings overseen by the Guro-gu district, the monitoring locations were carefully selected. The selection criteria included the ability to provide representative data, quality assurance, site security, power access, and specific building consideration. The SAMI network adhered to a neighborhood spatial scale, as specified by the U.S. EPA's five categories, with sensors spaced 0.5 to 4.0 km apart [27]. To assess the accuracy of 12 measuring instruments equipped with low-cost sensors, the study compared the $PM_{2.5}$ concentrations measured under identical conditions to those obtained from an ambient air monitoring station operated using the Federally Equivalent Methods in Riverside, California, USA [28]. The data collected from the six low-cost sensors showed a relatively high correlation, with R^2 values ranging from 0.7 to 0.75. Furthermore, during a field test conducted in Australia, a correlation analysis was performed by computing the daily average concentration of ambient $PM_{2.5}$ measured by an air quality monitoring station and a low-cost IoT sensor [29]. The results indicated a strong correlation between R^2 and the range of 0.63–0.87, which suggests a relatively high level of performance. Similar to the results by Feenstra et al. and Tagle et al. [28,29], the R^2 value of the predictive model in this study, which included SAMIs, showed a strong correlation ranging from 0.88 to 0.95.

The accuracy of estimating $PM_{2.5}$ concentration improved when SAMIs were used in combination with the AQMS compared with the results obtained through single-point interpolation when using only the AQMS. By estimating the AQMS using each spatial interpolation technique with Model 1 as a single point, the R^2 value was found to be 0.66. The accuracy improved significantly when SAMIs were installed as an auxiliary, increasing from approximately 23% to 55%. Moreover, the RMSE and MAE values were relatively low, indicating an increase in the accuracy of the model estimation of $PM_{2.5}$. One simulation study demonstrated that the accuracy of $PM_{2.5}$ concentration predictions decreased as the number of monitoring stations decreased from 22 to 12 [30]. In a study that evaluated the performance of a model estimating $PM_{2.5}$, the accuracy improved in cities with a higher number of monitoring stations compared with those with fewer monitoring stations. This suggests that the accuracy of concentration prediction improves as the number of monitoring stations increases, owing to the increase in spatial resolution density [31]. Furthermore, SAMIs can overcome spatial limitations and gather data from many locations [32]. This can improve the accuracy of predicting $PM_{2.5}$ concentrations and contribute to more precise assessments of exposure.

Seven stations (S_1–S_7) of the SAMIs were selected based on their distances from the AQMS. The estimated values were obtained through spatial interpolation and then compared to the observed values using statistical verification techniques. All four models (Models 1, 2, 3, and 4) showed that the R^2 value between the observation and estimation decreased with the distance from the installed AQMS. According to the installation and operation guidelines for AQMSs, the distance between air quality monitoring stations should be 2 km to avoid redundancy [33]. This suggests that the AQMS represents the

$PM_{2.5}$ concentration for an area within a radius of approximately 2 km and is not indicative of the concentration beyond this distance. SAMIs are considered to have spatial representativeness when the R^2 value is above 0.80 within a radius of approximately 1.5 km. Therefore, a clear estimation of unmeasured points was possible by installing SAMI at approximately 3 km intervals. The installation requirements for monitoring stations vary depending on the presence or absence of air pollutant sources. However, for large cities, such as Seoul, the accuracy of $PM_{2.5}$ concentration estimation could improve if measurement stations are installed at 3 km intervals. By comparing the statistical values of Models 3 and 4, it was observed that the R^2 value of Model 4 decreased. These results are contrary to the research direction, which stated that the accuracy of the $PM_{2.5}$ concentration estimation would increase with an increase in the number of monitoring stations. Owing to the nature of the interpolation technique, it is sensitive to points in close proximity. As a result, AQMSs located outside the Guro-gu district did not have a significant impact on the improvement in $PM_{2.5}$ concentration estimation. As the distance from the AQMS increased, the R^2 value between the observed and estimated values of the selected SAMIs decreased. Combining the AQMSs and SAMIs in a region could enhance the precision of $PM_{2.5}$ concentration estimations for unmeasured locations.

This study identified the limitations of AQMS in accurately measuring local $PM_{2.5}$ concentrations due to their restricted spatial coverage. By integrating SAMI, we were able to effectively address these shortcomings, specifically through the auxiliary installation of SAMIs, which significantly enhanced the spatial resolution and accuracy of $PM_{2.5}$ concentration estimations. Furthermore, our research established the optimal deployment range for SAMIs, ensuring effective spatial representativeness. However, the accuracy of the statistical verification for SAMI may be compromised because of the short duration of only 3 days. In addition, the measured outdoor $PM_{2.5}$ results may be biased due to missing values in the concentration data, and the study area was limited to the Guro-gu district, Seoul.

Despite these limitations, this study provides significant insights into improving air quality monitoring and demonstrates the potential of using SAMIs to enhance the accuracy and spatial resolution of $PM_{2.5}$ measurements. In future studies, extending the data collection period of SAMI would be essential to ensure sufficient data availability. Additionally, it could be necessary to collect and compare data from both urban and rural areas, as well as to gather data during significant air quality events, like yellow dust storms. Although the sensors used have a 2-year warranty, research should be carried out to detect sensor malfunctions and resulting data errors during the measurement period.

5. Conclusions

This study classified four models based on the increase in the number of monitoring stations. Using QGIS, interpolation techniques, such as IDW and kriging, were used to visualize the concentration, and statistical verification between the estimated concentration value and the observed value was performed. Based on the IDW, OK, and UK techniques in Model 3, the R^2 values were 0.88, 0.95, and 0.95, respectively. These values indicate a higher correlation than the results of the interpolation obtained using Model 1. In addition, compared with Model 1, the RMSE and MAE showed low values, indicating that the $PM_{2.5}$ concentration estimation model had high accuracy. Following the assessment of the ambient $PM_{2.5}$ concentration estimation accuracy using spatial interpolation techniques, it was observed that the kriging technique demonstrated a higher accuracy than the IDW technique in each model. When statistical verification was performed on the monitoring stations according to distance, R^2 decreased as the distance from the AQMS increased. This suggests that the auxiliary installation of a SAMI is necessary. Consequently, the spatial limitations and cost aspects of the AQMS can be supplemented through the SAMIs. This increase in spatial resolution would improve the accuracy of $PM_{2.5}$ concentration estimation for unmeasured points, resolve the concentration distribution imbalance in a specific space, and efficiently manage air quality. It is possible to calculate the exact amount

of $PM_{2.5}$ exposure due to the increase in the measurement density. Therefore, it can be used for accurate exposure and risk assessments of the entire population and subgroups.

Author Contributions: Conceptualization, J.S. and J.W.; methodology, J.S. and J.W.; software, J.S. and J.W.; validation, Y.C., S.L., D.K. (Daehwan Kim) and W.Y.; formal analysis, J.S. and J.W.; investigation, G.M., D.K. (Dongjun Kim) and S.L.; resources, W.Y.; data curation, D.K. (Daehwan Kim), S.L. and D.K. (Dongjun Kim); writing—original draft preparation, J.S. and J.W.; writing—review and editing, Y.C., G.M., D.K. (Daehwan Kim) and S.L.; visualization, J.S., J.W. and Y.C.; supervision, W.Y. All authors have read and agreed to the published version of the manuscript.

Funding: This work was supported by the Korea Environment Industry & Technology Institute through the Environmental Health Action Program funded by the Ministry of Environment (MOE) of the Republic of Korea [Grant number 2021003320001 and 2021003320008].

Institutional Review Board Statement: Not applicable.

Informed Consent Statement: Not applicable.

Data Availability Statement: The data will be made available on request in accordance with the permission of the local government of Guro-gu district, which is the target area of this study.

Conflicts of Interest: The authors declare no conflicts of interest.

References

1. WHO. New WHO Global Air Quality Guidelines Aim to Save Millions of Lives from Air Pollution. Copenhagen and Geneva: World Health Organization. 2021. Available online: https://www.who.int/news/item/22-09-2021-new-who-global-air-quality-guidelines-aim-to-save-millions-of-lives-from-air-pollution (accessed on 4 December 2023).
2. Cohen, A.J.; Brauer, M.; Burnett, R.; Anderson, H.R.; Frostad, J.; Estep, K.; Balakrishnan, K.; Brunekreef, B.; Dandona, L.; Dandona, R.; et al. Estimates and 25-year trends of the global burden of disease attributable to ambient air pollution: An analysis of data from the Global Burden of Diseases Study 2015. *Lancet* **2017**, *389*, 1907–1918. [CrossRef] [PubMed]
3. International Agency for Research on Cancer. Outdoor Air Pollution a Leading Environmental Cause of Cancer Deaths. PR 221—IARC: Outdoor Air Pollution a Leading Environmental Cause of Cancer Deaths (who.int). 2013. Available online: https://www.iarc.who.int/wp-content/uploads/2018/07/pr221_E.pdf (accessed on 22 September 2023).
4. Choe, J.; Lee, Y. A study on the impact of $PM_{2.5}$ emissions on respiratory diseases. *J. Environ.* **2015**, *23*, 155–172. [CrossRef]
5. Siregar, S.; Idiawati, N.; Pan, W.C.; Yu, K.P. Association between satellite-based estimates of long-term $PM_{2.5}$ exposure and cardiovascular disease: Evidence from the Indonesian Family Life Survey. *Environ. Sci. Pollut. Res.* **2022**, *29*, 21156–21165. [CrossRef] [PubMed]
6. Slawsky, E.; Ward-Caviness, C.K.; Neas, L.; Devlin, R.B.; Cascio, W.E.; Russell, A.G.; Huang, R.; Kraus, W.E.; Hauser, E.; Diaz-Sanchez, D.; et al. Evaluation of $PM_{2.5}$ air pollution sources and cardiovascular health. *Environ. Epidemiol.* **2021**, *5*, e157. [CrossRef] [PubMed]
7. Suryadhi, M.A.H.; Suryadhi, P.A.R.; Abudureyimu, K.; Ruma, I.M.W.; Calliope, A.S.; Wirawan, D.N.; Yorifuji, T. Exposure to particulate matter ($PM_{2.5}$) and prevalence of diabetes mellitus in Indonesia. *Environ. Int.* **2020**, *140*, 105603. [CrossRef] [PubMed]
8. Gulia, S.; Prasad, P.; Goyal, S.K.; Kumar, R. Sensor-based Wireless Air Quality Monitoring Network (SWAQMN)—A smart tool for urban air quality management. *Atmos. Pollut. Res.* **2020**, *9*, 1588–1597. [CrossRef]
9. Castell, N.; Dauge, F.R.; Schneider, P.; Vogt, M.; Lerner, U.; Fishbain, B.; Broday, D.; Bartonova, A. Can commercial low-cost sensor platforms contribute to air quality monitoring and exposure estimates? *Environ. Int.* **2017**, *99*, 293–302. [CrossRef] [PubMed]
10. Taştan, M.; Gökozan, H. Real-time monitoring of indoor air quality with internet of things-based e-nose. *Appl. Sci.* **2019**, *9*, 3435. [CrossRef]
11. Snyder, E.; Watkins, T.; Solomon, P.; Thoma, E.; Williams, R.; Hagler, G.; Shelow, D.; Hindin, D.; Kilaru, V.; Preuss, P. The changing paradigm of air pollution monitoring. *Environ. Sci. Technol.* **2013**, *47*, 11369–11377. [CrossRef]
12. Bi, J.; Carmona, N.; Blanco, M.N.; Gassett, A.J.; Seto, E.; Szpiro, A.A.; Larson, T.V.; Sampson, P.D.; Kaufman, J.D.; Sheppard, L. Publicly available low-cost sensor measurements for $PM_{2.5}$ exposure modeling: Guidance for monitor deployment and data selection. *Environ. Int.* **2022**, *158*, 106897. [CrossRef]
13. Dubey, R.; Patra, A.K.; Joshi, J.; Blankenberg, D.; Kolluru, S.S.R.; Madhu, B.; Raval, S. Evaluation of low-cost particulate matter sensors OPC N_2 and PM Nova for aerosol monitoring. *Atmos. Pollut. Res.* **2022**, *13*, 101335. [CrossRef]
14. Hofman, J.; Nikolaou, M.; Shantharam, S.P.; Stroobants, C.; Weijs, S.; Manna, V.P.L. Distant calibration of low-cost PM and NO_2 sensors; evidence from multiple sensor testbeds. *Atmos. Pollut. Res.* **2022**, *13*, 101246. [CrossRef]
15. Lai, W.I.; Chen, Y.Y.; Sun, J.H. Ensemble machine learning model for accurate air pollution detection using commercial gas sensors. *Sensors* **2022**, *22*, 4393. [CrossRef] [PubMed]
16. Yoo, S.; Kim, B. A decision-making model for adopting a cloud computing system. *Sustainability* **2018**, *10*, 2952. [CrossRef]

17. Park, J.; Ryu, H.; Kim, E.; Choe, Y.; Heo, J.; Lee, J.; Cho, S.; Sung, K.; Cho, M.; Yang, W. Assessment of $PM_{2.5}$ population exposure of a community using sensor-based air monitoring instruments and similar time-activity groups. *Atmos. Pollut. Res.* **2020**, *11*, 1971–1981. [CrossRef]
18. Frigge, M.; Hoaglin, D.; Iglewicz, B. Some implementations of the boxplot. *Am. Stat.* **1989**, *43*, 50–54. [CrossRef]
19. Do, K.; Yu, H.; Velasquez, J.; Grell-Brisk, M.; Smith, H.; Elvey, C. A data-driven approach for characterizing community scale air pollution exposure disparities in inland Southern California. *J. Aerosol. Sci.* **2021**, *152*, 105704. [CrossRef]
20. Alimissis, A.; Philippopoulos, K.; Deligiorgi, D. Spatial estimation of urban air pollution with the use of artificial neural network models. *Atmos. Environ.* **2018**, *191*, 205–213. [CrossRef]
21. Ahmed, S.O.; Mazloum, R.; Abou-Ali, H. Spatiotemporal interpolation of air pollutant in the Greater Cairo and the Delta, Egypt. *Environ. Res.* **2018**, *160*, 27–34. [CrossRef]
22. Kumar, A.; Mishra, R.K.; Sarma, K. Mapping spatial distribution of traffic induced criteria pollutants and associated health risks using kriging interpolation tool in Delhi. *J. Transp. Health* **2020**, *18*, 100879. [CrossRef]
23. Kang, D.; Bong, C.; Kim, D. Real-time high resolution PM monitoring in Seoul. Korean Assoc. *Part. Aerosol. Res.* **2019**, *15*, 67–78. [CrossRef]
24. Li, J.; Li, R.; Husain, T.; Khan, A.; Huang, Z. Spatial Interpolation of Fine Particulate Matter Concentrations Using the Shortest Wind-Field Path Distance. *PLoS ONE* **2014**, *9*, e96111. [CrossRef]
25. Wei, P.; Zhang, Y.; Meng, C. Spatial estimation of regional $PM_{2.5}$ concentrations with GWR models using PCA and RBF interpolation optimization. *Remote Sens.* **2022**, *14*, 5626. [CrossRef]
26. Karagulian, F.; Barbiere, M.; Kotsev, A.; Spinelle, L.; Gerboles, M.; Lagler, F.; Redon, N.; Crunaire, S.; Borowiak, A. Review of the performance of low-cost sensors for air quality monitoring. *Atmos* **2019**, *10*, 506. [CrossRef]
27. Washington State Department of Ecology. Air Monitoring Site Selection and Installation Procedure. 2019. Available online: https://fortress.wa.gov/ecy/publications/summarypages/1602021.html (accessed on 20 May 2024).
28. Freenstra, B.; Papapostolou, V.; Hasheminassab, S.; Zhang, H.; Boghossian, B.D.; Cocker, D.; Polidori, A. Performance evaluation of twelve low-cost $PM_{2.5}$ sensors at an ambient air monitoring sites. *Atmos. Environ.* **2019**, *216*, 116946. [CrossRef]
29. Tagle, M.; Rojas, F.; Reyes, F.; Vásquez, Y.; Hallgren, F.; Lindén, J.; Kolev, D.; Wante, Å.K. Field performance of a low-cost sensor in the monitoring of particulate matter in Santiago, Chile. *Environ. Monit. Assess.* **2020**, *192*, 171. [CrossRef]
30. Kim, S.; Sheppard, L.; Kim, H. Health effects of long-term air pollution influence of exposure prediction methods. *Epidemiology* **2009**, *20*, 442–450. [CrossRef] [PubMed]
31. Kim, S.; Yi, S.; Eum, Y.; Choi, H.; Shin, H.; Ryou, H.; Kim, H. Ordinary kriging approach to predicting long-term particulate matter concentrations in seven major Korean cities. *Environ. Health Toxicol.* **2014**, *29*, 12.1–12.8. [CrossRef]
32. Considine, E.M.; Reid, C.E.; Ogletree, M.R.; Dye, T. Improving accuracy of air pollution exposure measurements: Statistical correction of a municipal low-cost airborne particulate matter sensor network. *Environ. Pollut.* **2021**, *268*, 115833. [CrossRef]
33. Korean Ministry of Environment. Air Pollution Monitoring Network Installation and Operation Instructions. 2018. Available online: http://27.101.216.209/home/file/readFile.do;jsessionid=oUUJ9jiVXZOLQdODyJXiPkT9.mehome1?fileId=222422&fileSeq=3 (accessed on 11 September 2023).